VARIATIONS OF ATMOSPHERIC CHARACTERISTICS IN THE HIGH-LATITUDE REGION OF THE NORTHERN HEMISPHERE DURING SOLAR PROTON EVENTS JANUARY 2005

© 2025 S. V. Veretenenko[a], *, A. V. Koval[b]

[a]*A.F. Ioffe Institute of Physics and Technology, Russian Academy of Sciences, St. Petersburg, Russia*

[b]*St. Petersburg State University, St. Petersburg, Russia*

**e-mail: s.veretenenko@mail.ioffe.ru*

Received February 25, 2025

Revised February 25, 2025

Accepted June 17, 2025

Abstract. A study of atmospheric characteristics in the high latitudes of the Northern Hemisphere in connection with a powerful solar activity outburst during January 13-23, 2005 which caused a series of solar proton events, strong magnetic storms, and a deep Forbush depression of galactic cosmic rays has been carried out. It is shown that the studied outburst was accompanied by a significant perturbation of the middle and lower atmosphere of high latitudes. The largest changes in the stratospheric circulation (a sharp increase in the intensity of the stratospheric polar vortex) occurred on 15-19 January and coincided in time with a significant increase in the ionization rate in the upper stratosphere and mesosphere, an increase in the NAO (North Atlantic Oscillation) index and a weakening of wave activity. In the lower atmosphere during the period under study, an intensive regeneration of cyclones near the southeastern coast of Greenland was observed. The vortex intensification was accompanied with a significant decrease of temperature in the stratosphere (by~ 10 K) in the area of latitudes above 70º N. Further sharp weakening of the vortex at the end of January contributed to the beginning of the event close by characteristics to the sudden stratospheric warming. The results of the study suggest that a possible influence on the development of the observed disturbances was exerted by phenomena associated with a sharp increase in solar flare activity in the period 13-23 January 2005, including a series of powerful solar proton events that caused a significant increase in ionization in the middle atmosphere.

DOI: 10.31857/S00167940250708e1

1. INTRODUCTION

The middle of January 2005 was marked by a powerful burst of solar activity, which occurred during the deep phase of the solar cycle decline against the background of already rather quiet

conditions on the Sun. On January 13, 2005, a sharp intensification of flare activity began, which was observed through January 23 and led to solar proton events (SPEs) on January 15, 16, 17, and 20, powerful magnetic storms of the G3 and G4 classes on January 16-21, and a deep Forbush decrease in the intensity of galactic cosmic rays (GCRs). At the same time, the winter of 2004/2005 was characterized by a rather stable state of the atmosphere and a strong persistent stratospheric polar vortex (e.g., [Rosevall et al., 2008]). In this connection, the study of the response of a quiet stable atmosphere to extreme manifestations of solar activity is of great scientific interest and certainly requires comprehensive studies that take into account the contributions of various physical agents and related mechanisms of the influence of solar activity on the state of the atmosphere. In the present paper, we consider the changes in the atmospheric characteristics at high latitudes of the Northern Hemisphere observed in the period from mid-January to mid-February 2005 and discuss their possible connection with the indicated solar activity burst.

2. EXPERIMENTAL DATA AND THEIR ANALYSIS

2.1 Variations of heliogeophysical characteristics in connection with the solar flare outburst in 2005

During the period from January 13 to 23, 2005, there was a significant increase in flare activity on the Sun. Figure 1a shows the time course of the Kleecek flare index, which characterizes the total energy released by a flare (e.g., [Özgüç et al, 2003]), and the number (per day) of X-ray flares of classes C, M, and X. Flares M8.6 and X2.6 (January 15), X3.8 (January 17), and X7.1 (January 20) led to significant increases in the solar proton flux in Earth's orbit - solar proton events on January 15, 16, 17, and 20 [Logachev et al., 2016]. During all events, particles with energies >100 MeV were recorded (Fig. 1b), sufficient for the particles to reach stratospheric heights (~ 32 km and below). The January 17 and 20 events also saw an increase in the flux of particles with energies >500 MeV reaching heights~ 15 km and involved in nuclear interactions, leading to increases in the neutron monitor count rate, i.e., Ground Level Enhancement events GLE-68 and GLE-69, respectively [Logachev et al., 2016]. The January 20 event is the second most powerful after GLE-5 on 23.02.1956. The event characteristics (onset, duration, maximum proton fluxes $F_{max}$with energies >10 MeV and >100 MeV, source on the Sun) are given in Table. The investigated series of PCA led to a significant increase in ionization in the polar atmosphere. Fig. 1c shows the mean daily values of the ionization rate in the region of geomagnetic latitudes 60-90º according to the data of the SOLARIS-HEPPA international working group. It can be seen that the largest changes in the ionization rate (> 1000 $cm^{-3} \cdot s^{-1}$) occurred in the mesosphere above the isobaric level of 1 hPa **(**heights greater than50 km) on 16-18 January. Ionization rates due to the GLE-69 event reached a maximum (~ 800 $cm^{-3} \cdot s^{-1}$) in the region from 10 to~ 1 hPa (altitudes~ 30-50 km) on 20 January.

Large coronal mass ejections (CMEs) are associated with the outburst, which caused strong magnetic storms of the G3 and G4 levels from January 16 to 21 (https://xras.ru/magnetic_storms.html?m=1&y=2005&r= moskva). Figure 1d shows a sharp increase ofΣ Kp (sum per day of the planetary geomagnetic perturbation index) on January 17, which reached a maximum (47.3) on January 18. At high latitudes, a significant intensification of auroral activity was observed when the geomagnetic AE-index characterizing the intensity of auroral phenomena reached the maximum values~ 1200-2000 nT (Fig. 1e). The magnetic storms were accompanied with a series of Forbush decreases of the GCR intensity. According to the data of the neutron monitor in Calgary (stiffness of the geomagnetic cutoff R= 1.09 GW), shown in Fig. 1f, the total amplitude of the Forbush decreases was~ 16% relative to the undisturbed level on January 13-16 according to mean daily data, with the minimum of the count rate observed on January 19. On January 20, a sharp increase in the count rate due to GLE-69 was registered (Fig. 1f).

Thus, the above data show that in the middle of January 2005, a rather rare complex of powerful heliogeophysical phenomena was observed due to a sharp burst of flare activity during the decline phase of the 23rd solar cycle.

2.2 Variations of the characteristics of the high-latitudinal middle atmosphere in January 2005

The MERRA-2 (Modern Era Retrospective analysis for Research and Applications, version 2) reanalysis archives [Gelaro et al., 2017], covering the altitude range from 1000 to 0.1 hPa, were used as an experimental base for investigating the atmospheric characteristics during the mid-January events 2005. Special attention was paid to the state of the stratospheric polar vortex, which appears to play an important role in solar-climate coupling [Veretenenko, 2022]. The mean daily values of the zonal (directed along the latitude circle) wind speed component in the stratosphere were used to characterize the vortex intensity.

Figure 2 shows maps of the distribution of zonal wind speed U (positive west-to-east direction) at 50 hPa for calm conditions before the onset of the outburst (January 12), on the day of the first event of the PCA series (January 15), a few days after the onset of the outburst (January 17 and 19), the day after the GLE-69 event (January 21), and at the end of the month (about 2.5 weeks after the onset of the outburst). The polar vortex is visible on the maps as an area of sharp increase in zonal wind at latitudes 50-80° N. The area where wind speeds exceed 40 $m \cdot s^{-1}$ is highlighted in dark brown. White asterisks indicate points of maximum wind speed values. The data in Fig. 2 show that there was a marked increase in zonal wind speed in the vortex region during the outburst. A significant increase in the area covered by winds with U> 40 $m \cdot s^{-1}$, both in longitude and area, can be seen. While before the outburst this area was localized mainly over the Arctic coast of North

America, a few days later it already extended over the North Atlantic and Scandinavia, with the maximum wind speeds significantly increased and shifted to the east. Thus, the presented data indicate a significant increase of wind speed in the vortex over the North Atlantic region during the investigated events. After January 20, the area of strong winds began to break up, with the southern boundary of the vortex in the region of longitudes 0-80ºE shifted to low latitudes (Fig. 2f).

The temporal variations (deviations from linear trends) of the maximum values of zonal wind speed in the region of latitudes 50-80ºN (the area of polar vortex formation) in January 2005 are shown in Fig. 3 for different isobaric levels. 3 for different isobaric levels. One can see that in the middle of January there was a sharp increase of the maximum wind speed at the levels from 70 to~ 1-2 hPa (the region of altitudes~ 18-50 km), which indicates the intensification of the stratospheric polar vortex. Comparison with the data in Fig. 1c shows that the onset of vortex intensification coincided in time with a sharp increase in flare activity and a significant increase in the ionization rate (> 1000 $cm^{-3} \cdot s^{-1}$) in the mesosphere above the 1 hPa level due to solar proton events. The largest increase in zonal wind speed (at~ 20-24 $m \cdot s^{-1}$relative to the linear trend) was observed at levels of 10-7 hPa (~ 30-33 km) on January 18-19. After 20 January, the maximum values of zonal wind speed in the vortex began to decrease despite the increase of the ionization rate during the GLE-69 event.

Fig. 4a presents the time course of zonal-averaged (averaged along the latitude circle) values of zonal wind speed (after subtracting the linear trend) at the isobaric level of 7 hPa, where the largest vortex intensification was detected during the solar activity burst. It can be seen that the zonal wind speed in the region of latitudes 50-70ºN during the period from January 15 to 25, which includes a complex of powerful heliogeophysical phenomena, increases significantly. The largest deviations of the wind speed from the trend values are as follows (at~ 25 $m \cdot s^{-1}$) were observed at the latitudes~ 60-64ºN. As can be seen from Fig. 4b, the intensification of the polar vortex in the indicated period caused the temperature decrease (by~ 8-10 K relative to a linear trend) in the area of latitudes> 60ºN, determined by the decrease of heat exchange between high and middle latitudes.

The data in Fig. 4a show that a sharp increase of the polar vortex in the period 15- January 25 was followed by its significant weakening in late January - early February (decrease of zonal wind speed by~ 15 $m \cdot s^{-1}$relative to the trend values). The vortex weakening was accompanied by a significant and rapid increase of stratospheric temperature (Fig. 4b) in the region of latitudes >70ºN (by~ 10-12 K relative to the linear trend and by~ 15-25 K relative to the minimum values observed during the outburst period). Maps of the zonal wind speed distribution in the stratosphere (Fig. 2) show that in late January there was both a decrease in the wind speed in the vortex and a change in

its shape– transition from a symmetric annular shape in mid-January (Fig. 2 a-d) to a strongly elongated one, with a significant displacement of the southern boundary of the vortex to latitude~ 40ºN in the region of longitudes 0-80ºE (Fig. 2f). Weakening of the vortex accompanied by a change in its shape, as well as a rapid temperature increase (by~ 15-25 K during the last week of January in the upper high-latitude stratosphere) indicate the development of a process close in its properties to a small sudden stratospheric warming.

2.3 Processes in the lower atmosphere in January 2005

As shown by the analysis of synoptic charts, simultaneously with the vortex intensification in the stratosphere, an intensive deepening of cyclones near the southeastern coast of Greenland was observed in the lower atmosphere in the period from January 15 to 17. On the synoptic map of January 15 (Fig. 5a), one can see two occluded (i.e., having reached the stage of maximum development) cyclones with pressure at the centers of 979 and 990 hPa near the southwestern and southeastern coasts of Greenland, respectively. One can see on the map on January 17 that the indicated cyclones moved to the northeastern direction and sharply deepened: the area covered by the closed isobars (cyclonic circulation) increased significantly and the pressure at the cyclone centers decreased by 35 hPa to 944 and 955 hPa, respectively. The process of secondary deepening of cyclones that have reached the stage of maximum development is called regeneration [Vorobyev, 1991] and is characteristic of the southeastern coast of Greenland, where the presence of a glacial surface promotes advection of cold air to the rear of the cyclone (a necessary condition for regeneration). According to [Veretenenko and Thejll, 2004], more intensive regeneration of cyclones near the southeastern coast of Greenland takes place after the onset of the SPE with particle energies > 90 MeV (sufficient to reach the level of the upper stratosphere). A comparative analysis of cyclone evolution in [Veretenenko and Tyle, 2008] showed that after the onset of the SPE, cyclones in the indicated region deepen more often, and the pressure in them decreases more than under unperturbed conditions. On the days following the SPE, the cyclones deepening by 10-15 hPa is most probable (on quiet days - by 5 hPa) and one can also observe cases of significant pressure decrease by 20-45 hPa. Thus, an intensive regeneration of cyclones (with a pressure decrease in the center by 35 hPa) detected during the period of the investigated series of SPEs agrees with the previously obtained results.

The intensive secondary deepening of cyclones near the coast of Greenland observed after the beginning of the solar activity burst and a series of SPEs was accompanied with a sharp increase of the NAO (North Atlantic Oscillation) index characterizing the pressure gradient between high and subtropical latitudes and the intensity of zonal circulation over the North Atlantic [Hurrel et al., 2003]. Fig. 6 shows the time course of the NAO index (after subtracting the linear trend) from the data (https://psl.noaa.gov/data/timeseries/daily/NAO/). The index was calculated as the difference

of 500 hPa geopotential heights averaged with area weighting over the 35-45ºN, 70-10ºW and 55-70ºN, 70-10ºW regions (relative to climatic values for 1981-2010). One can see a significant increase of the NAO index in the period from January 15 to 20 and a noticeable decrease in the subsequent period (January 22-27). The indicated changes in the intensity of zonal circulation over the North Atlantic described by the NAO index agree with the previously detected changes of zonal circulation in temperate latitudes characterized by the Blinova index due to variations of cosmic rays [Veretenenko and Pudovkin, 1993]. According to the results of this work, solar proton events with particle energies > 90 MeV are accompanied by a marked strengthening of the zonal circulation, whereas Forbush decreases of the GCR cause its weakening. The NAO variations revealed a high correlation (R~ 0.8) with the maximum values of the zonal wind speed U_{max} at 70 hPa (Fig. 6).

As discussed above, the intensification of zonal wind in the stratosphere during the time interval between January 15 and 25, coincided in time with the period of solar activity burst. In addition, it was accompanied with a significant weakening of wave activity in the middle atmosphere. Planetary waves (PV) are global fluctuations of atmospheric parameters (pressure, density, temperature) covering the entire thickness of the atmosphere (e.g., Holton, 2004). They originate in the lower atmosphere and propagate to the uppermost layers, with the amplitude of the oscillations increasing with altitude due to decreasing atmospheric density. In the free atmosphere, above the tropopause, the SPs represent the dominant form of motion, determining the energy and momentum transfer between different layers of the atmosphere.

In Fig. 7 shows the amplitudes of planetary waves with zonal number 1 and 2 at latitude 62ºN, corresponding to the axis of the zonal jet stream. The prolonged (>10 days) weakening of wave 1 (Fig. 7a) is especially pronounced, while wave 2 first sharply weakens and then begins to gradually strengthen already on the third day (Fig. 7b) after the beginning of the series of PCA. The momentum transfer itself between the SP and the background current is absolutely typical: the intensification of the jet stream (in our case, the stratospheric polar vortex) is usually accompanied by a divergence of the wave activity flux, i.e., a momentum transfer from the collapsing planetary wave (e.g., Holton, 2004; Koval et al., 2025). However, it is important to consider the accompanying dynamical processes here.

In Fig. 8a, the filling represents the time course of the zonal wind in the latitudinal interval 52° -77° N, and the contours represent the meridional thermal gradient. According to the classical "thermal wind" theory (e.g., Gill, 1982), the vertical gradient of the zonal (meridional) wind is proportional to the meridional (zonal) temperature gradient. Polar stratospheric cooling, the mechanisms of which are discussed in the next section, explains the increase in the meridional temperature gradient observed in Fig. 8a during times of increased solar activity (labeled in Fig. 8

with vertical lines). It is this increase in the meridional gradient that causes an increase in the vertical gradient of the zonal wind, accelerating the polar vortex. The associated changes in the wave characteristics of the atmosphere accompanying the change in the SP amplitudes in Fig. 7 and polar vortex velocity in Fig. 8a are presented in Fig. 8b. The fill in Fig. 8b represents the vertical component of the Eliassen-Palm wave activity vector (EP flux), which characterizes the propagation intensity of the SP wave activity and illustrates the momentum exchange between the wave and the zonal flow (Jucker, 2021; Koval et al., 2025). The pattern of the EF flux generally corresponds to the variation of SP amplitudes in Fig. 7. The contours represent the time course of the divergence of the Eliassen-Palm wave activity flux. The divergence of the EF flux is usually interpreted as a transfer of momentum from the wave to the background flux accompanied by a positive (eastward-directed) acceleration of the zonal wind. At the end of the phase of solar activity intensification, January 22-23, in Fig. 8b below 30 km, one can observe the intensification of the reverse process - negative divergence (i.e., convergence) of the ES flux, which characterizes the reverse transfer of the impulse from the polar vortex to the planetary wave. Further, we observe an increase in wave activity - strengthening of the vertical component of the ES flux (fill in Fig. 8b). Thus, one can assume that the spatial structure of pressure variations in the troposphere, which was created by mid-January and determined, in particular, by the cyclonic processes discussed above, could contribute to the enhanced generation of EP. In turn, these wave structures rapidly developed at the expense of pumping the impulse from the background flow, simultaneously weakening the zonal circulation, which is indirectly confirmed by the corresponding changes of divergence of the EF flux. Further intensification of wave activity and weakening of the zonal wind contributed to heating of the polar stratosphere and formation by the end of January of a dynamic structure close to the characteristics of the sudden stratospheric warming

3. DISCUSSION OF THE RESULTS

The results of the study show that from mid-January to early February 2005, the entire high-latitude atmosphere from the troposphere to the mesosphere was perturbed. During the period of the solar activity burst from January 13 to 23, including intensification of flare activity, a series of powerful solar proton events, intense geomagnetic storms and auroral activity, a number of different atmospheric phenomena were observed. In the middle atmosphere, there was a sharp intensification of the stratospheric polar vortex, which caused a significant temperature decrease in the polar middle atmosphere. In the lower atmosphere, one observed an intensive regeneration of the North Atlantic cyclones, a significant intensification of zonal circulation characterized by the NAO index and weakening of wave activity. A possible influence on the development of the indicated processes could be exerted by heliogeophysical phenomena determined by the solar activity burst.

The presence of a number of solar-conditioned factors acting almost simultaneously allows us

to assume the operation of different physical mechanisms of the influence of solar activity on the atmospheric circulation. First of all, one should note the changes in the ionization rate determined by variations of energetic charged particles. A review of the geophysical effects of ionization rate increases due to the SPE, including changes in the chemical composition of the polar atmosphere (ozone layer depletion), perturbations in the global electric circuit, nitrate formation, changes in atmospheric transparency, etc., can be found in [Miroshnichenko, 2008]. During the investigated solar activity burst, there was an increase in the fluxes of energetic solar protons, which caused a significant increase in the ionization rate in the mesosphere and upper and middle stratosphere (Fig. 1c). A deep Forbush decrease in the flux of galactic cosmic rays was also observed (Fig. 1f), causing a decrease in the ionization rate in the lower stratosphere and upper troposphere at heights~ 10-20 km [Bazilevskaya et al., 2008]. At high latitudes, there was a significant increase of auroral activity (Fig. 1e), indicating an increase of ionization in the polar atmosphere due to the ejections of low-energy (1-30 keV) auroral electrons. The electron energy is absorbed mainly at the lower thermosphere heights (above 90 km). At the same time, electron ejections contribute to the generation of braking X-ray radiation capable of penetrating to stratospheric heights and causing changes in the ionization rate [Jackman, 1991].

The important role of the ionization rate in the mechanism of solar-atmospheric coupling is indicated by the differences in the response of the lower atmosphere to variations of cosmic rays of different sign. According to [Veretenenko and Pudovkin, 1993], opposite in sign variations of the zonal circulation are observed during the bursts of energetic solar protons and Forbush decreases of GCR, causing an increase and decrease of the ionization rate in the atmosphere, respectively. Also at the increase of the ionization rate during SPEs with energies >90 MeV, a more intensive cyclone regeneration and pressure decrease in the region of latitudes >50ºN in the North Atlantic are observed [Veretenenko and Thejll, 2004]. At the decrease of the ionization rate during the Forbush decreases of the GCR, a more intensive formation of blocking anticyclones and pressure growth over Northern Europe and the northern part of the European territory of Russia were detected [Artamonova and Veretenenko, 2011]. The intensification of anticyclonic processes (pressure growth) during the Forbush-declines of the GCR was detected over Western Siberia (Novosibirsk area) [Yanchukovsky, 2024]. A comparative analysis of the effects of PCA and Forbush-GCR decreases in the evolution of extratropical baric systems was carried out in [Veretenenko, 2017].

Related to changes in the ionization rate are mechanisms involving changes in the chemical composition of the mean polar atmosphere (ozone destruction) [Baumgaertner et al., 2011; Rozanov et al., 2012] and electrical mechanisms involving changes in the atmospheric conductivity and the density of vertical electric currents [Tinsley, 2008, 2022]. Since solar proton fluxes are characterized by a rapidly decreasing energy spectrum, the region of invasion of these particles is

limited to polar latitudes. The increase in the ionization rate in this region promotes a more intensive formation of the families of odd nitrogen $NO_x$and hydrogen HO_x, which catalytically destroy ozone [Rusch et al., 1981; Solomon et al., 1981]. Decreases in ozone content have been observed for a large number of powerful PCAs, beginning with the November 2 event 1969 [Weeks et al., 1972]. According to [Jackman et al., 2011], a series of SPEs of January 2005 caused a decrease of ozone content in the mesosphere and upper stratosphere in the 60-82.5ºN region by~ 60-70% and~ 10%, respectively, during the period January 16-24. Under polar night conditions (absence of solar radiation), ozone contributes to heating of the middle atmosphere by absorbing the outgoing long-wave radiation from the Earth and the underlying atmosphere. Thus, ozone destruction during the SPE can lead to cooling of the polar atmosphere, affecting the temperature distribution in the high-latitudinal middle atmosphere and the intensity of winds.

Changes in the ionization rate also affect the atmospheric conductivity and the density of vertical electric currents J_z, which contributes to the electrification of cloud particles and a more intensive course of microphysical processes in clouds [Tinsley, 2008, 2022]. In turn, changes in the state of clouds in winter can affect the fluxes of outgoing longwave radiation and the temperature regime of the high-latitude atmosphere. One of the possible consequences of cloud formation at the growth of $J_z$may be the release of latent heat contributing to the intensification of extratropical cyclones [Tinsley, 2012]. The intensification of cyclone regeneration near the Earth's surface observed with increasing ionization rates in the stratosphere and mesosphere suggests, apparently, an indirect influence of the ionization rate on the processes in the lower atmosphere, which may include variations in the electric current density.

It should be noted that the largest perturbation of the middle and lower atmosphere occurred during the period January 15-19, prior to the GLE-69 event. In spite of the fact that during this GLE the ionization rates increased at lower levels compared to the previous events, it did not lead to an intensification of the previously observed effects. On the contrary, it was followed by a sharp weakening of the polar vortex and a decrease in the NAO index. A possible reason is that the GLE growth occurred at the background of a strong deepening Forbush decrease of the GCL, contributing to the decrease of the ionization rate in the lower stratosphere and upper troposphere. In addition, the vortex weakening was facilitated by the increased wave activity (see Section 2.3).

It should be noted that following the burst of solar activity and related geophysical phenomena that occurred in the middle of January 2005, processes similar to the processes at sudden stratospheric warming (vortex weakening and change of vortex shape, sharp temperature increase) developed in the stratosphere of high latitudes at the end of the month. This allows us to make an assumption about a possible influence of events related to solar activity on the development of sudden stratospheric warming. Nevertheless, this assumption requires further

research.

4. CONCLUSIONS

The results of the study showed the following.

1) In the middle of January 2005 in the middle and lower high-latitudinal atmosphere, significant perturbations of large-scale circulation were observed including a sharp intensification of the stratospheric polar vortex, intensive regeneration of cyclones near the shores of Greenland, intensification of the NAO index and weakening of wave activity. The indicated perturbations were followed by vortex weakening, increased wave activity in the middle atmosphere and development of a small stratospheric warming.

2) A possible influence on the development of the atmospheric perturbations observed in the second half of January-early February, had a heliogeophysical phenomena connected with a sharp increase of flare activity on the Sun in the period January 13-23, 2005: a series of powerful solar proton events, intense magnetic storms accompanied with a deep Forbush decrease of the GCR, intensification of auroral activity.

3) The intensification of the polar vortex, which coincided in time with the increase of solar flare activity, is explained by the increase of the meridional thermal gradient, in turn caused by the cooling of the polar stratosphere. Simultaneously with the vortex intensification, intensification of cyclones in the North Atlantic and an increase of the NAO index were observed, which, in turn, contributed to the enhanced generation of planetary waves, leading to the weakening of the polar vortex and the occurrence of a weak sudden stratospheric warming in late January.

4) The results obtained imply the influence of changes in the ionization rate due to variations of energetic charged particles on the dynamics and temperature regime of the high-latitude middle atmosphere and on the processes in the lower atmosphere. The physical mechanism of this interaction seems to be based on changes in the temperature regime of the polar atmosphere, which occurred as a result of changes in its chemical composition, as well as changes in the cloud state due to enhanced vertical electric currents.

ACKNOWLEDGEMENT

Cosmic ray fluxes in the stratosphere were taken from the website of the P.N. Lebedev Physical Institute, Laboratory of Solar and Cosmic Ray Physics https://sites.lebedev.ru/. Ionization rates were obtained from the SOLARIS-HEPPA international working group website https://solarisheppa.geomar.de/solarprotonfluxes. We express our gratitude to them.

CONFLICT OF INTERESTS

The authors declare that they have no conflict of interest.

REFERENCES

1. *Veretenenko S.V.* Comparative analysis of short-term effects of solar and galactic cosmic rays in the evolution of baric systems of temperate latitudes // Izvestiya RAS. Physical series. V. 81. No. 2. P. 281-284. 2017.
2. *Veretenenko S.V., Pudovkin M.I.* Effects of cosmic ray variations in the circulation of the lower atmosphere // Geomagnetism and aeronomy. V. 33. No. 6. P. 35-40. 1993.
3. *Veretenenko S.V., Tile P.* Solar proton events and the evolution of cyclones in the North Atlantic // Geomagnetism and aeronomy. V. 48. No. 4. P. 542-552. 2008.
4. *Vorobyov V.I.* Synoptic Meteorology. L.: Hydrometeoizdat, 1991.
5. *Yanchukovsky V.L.* Reaction of the mid-latitude atmosphere to sporadic variations of cosmic rays in the region of Western Siberia // Solar-terrestrial Physics. V. 10. № 4. P. 65-71. 2024.
6. *Artamonova I., Veretenenko S.* Galactic cosmic ray variation influence on baric system dynamics at middle latitudes // J. Atmos. Solar-Terr. Phys. V. 73. No 2/3. P. 366-370. 2011.
7. *Baumgaertner A.J.G., Seppälä A., Jöckel P., Clilverd M.A.* Geomagnetic activity related NOx enhancements and polar surface air temperature variability in a chemistry climate model: Modulation of the NAM index // Atmos. Chem. Phys. V. 11. P. 4521–4531. 2011.
8. *Bazilevskaya G.A., Usoskin I.G., Fluckiger E.O. et al.* Cosmic Ray Induced Ion Production in the Atmosphere // Space Science Review. V. 137(1-4). P. 149-173. 2008.
9. *Gelaro R., McCarty W., Suarez M.J. et al.* The Modern-Era Retrospective Analysis for Research and Applications, Version 2 (MERRA-2) // J. Climate. V. 30. P. 5419-5454. 2017.
10. *Gill A.E.* Atmosphere-Ocean Dynamics. Academic Press, 1982
11. *Holton J.R.* An introduction to dynamic meteorology (fourth edition). New York: Elsevier Academic Press. 2004.
12. *Hurrell J. W., Kushnir Y., Ottersen, G., Visbeck M.* An overview of the North Atlantic Oscillation. In: The North Atlantic Oscillation: Climatic Significance and Environmental Impact. Geophysical Monograph Series. P. 1–35. 2003.
13. *Jackman C.H.* Effects of energetic particles on minor constituents of the middle atmosphere // J. Geomag. Geoelectr. V. 43. Suppl. P. 637-646. 1991
14. *Jackman C.H., Marsh D.R., Vitt F.M. et al.* Northern Hemisphere atmospheric influence of the solar proton events and ground level enhancement in January 2005 // Atmos. Chem. Phys. V. 11. P. 6153-6166. 2011.
15. *Jucker M.* Scaling of Eliassen-Palm flux vectors // Atmos. Sci. Lett. V. 22. No 4. e1020. 2021.
16. *Koval A.V., Didenko K.A., Ermakova T.S. et al.* Diagnostics of the solar activity influence on the global atmospheric circulation in the thermosphere and MLT area: wave—mean flow

interaction effects // Climate Dynamics. V. 63. 19. 2025.

17. *Logachev Yu.I., Bazilevskaya G.A., Vashenyuk E.V. et al.* Catalogue of Solar Proton Events in the 23rd Cycle of Solar Activity (1996-2008). Moscow: 2016. http://www.wdcb.ru/stp/data/SPE/Catalog_SPE_23_cycle_SA.pdf
18. *Miroshnichenko L.I.* Solar cosmic rays in the system of solar–terrestrial relations // J. Atm. Sol.-Terr. Phys. V. 70. P. 450-466. 2008.
19. *Özgüç A., Ataç T., Rybák J.* Temporal variability of the flare index (1996-2001) // Solar Phys. V. 214. P. 375-396. 2003.
20. *Rozanov E., Calisto M., Egorova T., Peter T., Schmutz W.* Influence of the precipitating energetic particles on atmospheric chemistry and climate // Surv. Geophys. V. 33. P. 483-501. 2012.
21. *Rösevall J.D., Murtagh D.P., Urban J. et al.* A study of ozone depletion in the 2004/2005 Arctic winter based on data from Odin/SMR and Aura/MLS // J. Geophys. Res. V. 113. D13301. 2008.
22. *Rusch D.W., Gérard J.-C., Solomon S., et al.* The effect of particle precipitation events on the neutral and ion chemistry of the middle atmosphere I. Odd nitrogen // Planet. Space Sci. V. 29. No 7. P. 767-774. 1981.
23. *Solomon S., Rusch D.W., Gérard J.-C., et al.* The effect of particle precipitation events on the neutral and ion chemistry of the middle atmosphere: II. Odd hydrogen // Planet. Space Sci. V. 29. No 8. P. 885-893. 1981.
24. *Tinsley B.A.* The global atmospheric electric circuit and its effects on cloud microphysics // Reports on Progress in Physics. V. 71. No 6. P. 66801-66900. 2008.
25. *Tinsley B.A.* A working hypothesis for connections between electrically-induced changes in cloud microphysics and storm vorticity, with possible effects on circulation // Adv. Space Res. V. 50. P. 791-805. 2012.
26. *Tinsley B.A.* Uncertainties in evaluating global electric circuit interactions with atmospheric clouds and aerosols, and consequences for radiation and dynamics // J. Geophys. Res. V. 127. e2021D035954. 2022.
27. *Veretenenko S.V.* Stratospheric polar vortex as an important link between the lower atmosphere circulation and solar activity // Atmosphere. V. 13. No 7. Art No 1132. 2022.
28. *Veretenenko S.* Thejll P. Effects of energetic solar proton events on the cyclone development in the North Atlantic // J. Atm. Sol.-Terr. Phys. V. 66. P. 393-405. 2004.
29. *Weeks L.H., Cuikay R.S., Corbin J.R.* Ozone measurements in the mesosphere during the solar proton event of 2 November 1969 // J. Atmos. Sci. V. 29. P. 1138-1142. 1972.

Table. Characteristics of solar proton events of January 2005 according to the catalog data [Logachev et al., 2016].

SPS	Onset (UT)	Duration, days	F_{max} (>10 MeV), $cm^{-2} \cdot s^{-1} \cdot sr^{-1}$	F_{max} (>100 MeV), $cm^{-2} \cdot s^{-1} \cdot s^{-1} \cdot sr^{-1}$	Source on the Sun
15.01.2005	07	1	7.4	0.11	M8.6/SF
16.01.2005	00	1.5	330	0.52	X2.6/3B
17.01.2005	13	2	3820	2.6	X3.8/3N
20.01.2005	06	4	1310	490	X7.1/2B

FIGURE CAPTIONS

Fig. 1. Variations of solar-geophysical characteristics in January 2005. a) Number (per day) of X-ray flares of the C class (gray-blue background) and the total number of flares of the M and X classes (blue background) according to the data (https://www.ngdc.noaa.gov/stp/space-weather/solar-data/solar-features/solar-flares/x-rays/goes/xrs/). The thick red line shows the time course of the Kleecek index (http://www.koeri.boun.edu.tr/astronomy/fi_nedir.htm). (b) Time course of integrated proton fluxes with energies >5, >50, and >100 MeV from GOES-11 data (https://www.swpc.noaa.gov/products/goes-proton-flux/). (c) Daily averages of the ionization rate ($cm^{-3} \cdot s^{-1}$) in the middle atmosphere in the region of geomagnetic latitudes 60-90º from SOLARIS-HEPPA data (https://solarisheppa.geomar.de/solarprotonfluxes). (d) Time course of the planetary geomagnetic disturbance indexΣ Kp (sum for a day) (http://www.wdcb.ru/stp/geomag/geomagn_Kp_ap_Ap_ind.ru.html). (e) Time course of the AE index (http://www.wdcb.ru/stp/geomag/geomagn_AE_AU_AL_AO_ind.ru.html). (f) Time course of the count rate of the neutron monitor in Calgary (geomagnetic latitude F ~ 58º, geomagnetic clipping hardness R_S= 1.09 GV) (http://cr0.izmiran.ru/calg/main.htm).

Fig. 2. Zonal wind speed (in $m \cdot s^{-1}$) at the stratospheric level of 50 hPa in January 2005: (a) before the outburst (January 12); (b) on the day of the start of the PCA series (January 15); (c and d) during the PCA series: January 17 and 19; (e) the day after GLE-69 (January 21);. (f) 2.5 weeks after the start of the ATP series (January 31). The area where wind speeds exceed 40 $m \cdot s^{-1}$ is highlighted in dark. White asterisks indicate the points of maximum zonal wind speeds.

Fig. 3. Variations (deviations from linear trends) of maximum values of zonal wind speed ($m \cdot s^{-1}$) at different stratospheric levels in the region of latitudes 50-80ºN in January 2005.

Fig. 4. a) Variations (deviations from linear trends) of zonal-averaged values of zonal wind speed

($m \cdot s^{-1}$) at different latitudes in January-February 2005 (isobaric level 7 hPa); (b) Variations (deviations from linear trends) of zonal-averaged values of temperature (K) at different latitudes in January-February 2005 (isobaric level of 7 hPa).

Fig. 5. Secondary deepening of cyclones off the coast of Greenland during the January 15-20 SPS series 2005: (a) position of cyclones on the synoptic map on January 15, 2005 (00UT); (b) The same on January 17, 2005 (00UT) according to (https://www.metoffice.gov.uk).

Fig. 6. Variations (deviations from linear trends) of the NAO index (red solid line) and maximum values of zonal wind speed U_{max} at the 70 hPa isobaric level (blue dashed line) in January 2005.

Fig. 7. Time course of the amplitude of geopotential height variations (in hp. m) caused by planetary waves with wave numbers 1 (a) and 2 (b) at latitude 62ºN in January 2005.

Fig. 8. Time course of: (a) zonal wind (m/s, fill) and meridional thermal gradient (K/rad, contours) averaged over the latitude interval 52º-72ºN (a); (b) vertical component of EF flux (fill, m^2/s^2) and EF flux divergence (contours, m/s/d).

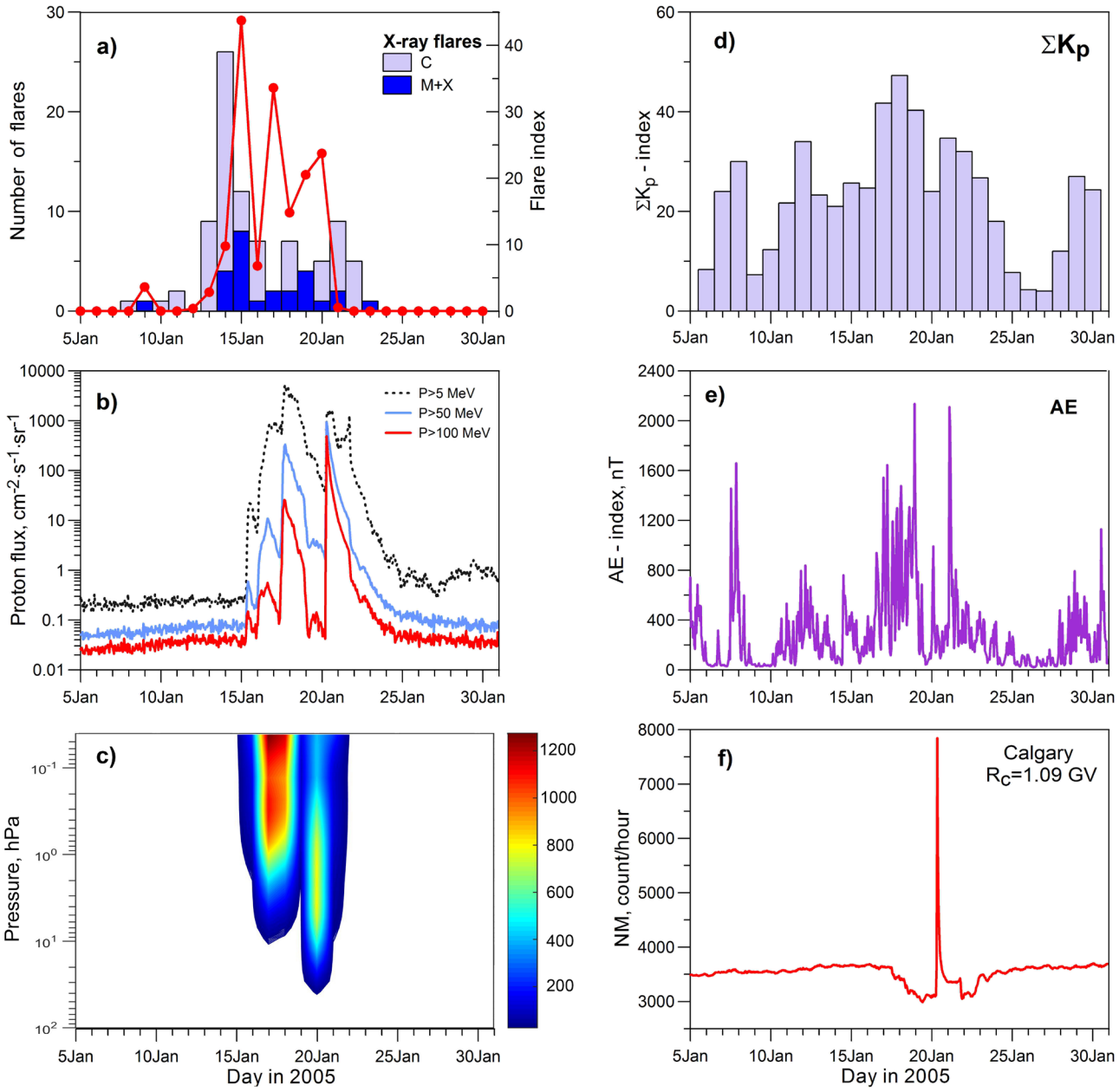
a)
X-ray flares
C
M+X
Number of flares
Flare index
b)
P>5 MeV
P>50 MeV
P>100 MeV
Proton flux, cm-2·s-1·sr-1
c)
Pressure, hPa
d)
ΣKp
ΣKp - index
e)
AE
AE - index, nT
f)
Calgary
Rc=1.09 GV
NM, count/hour
5Jan
10Jan
15Jan
20Jan
25Jan
30Jan
Day in 2005

Fig. 1.

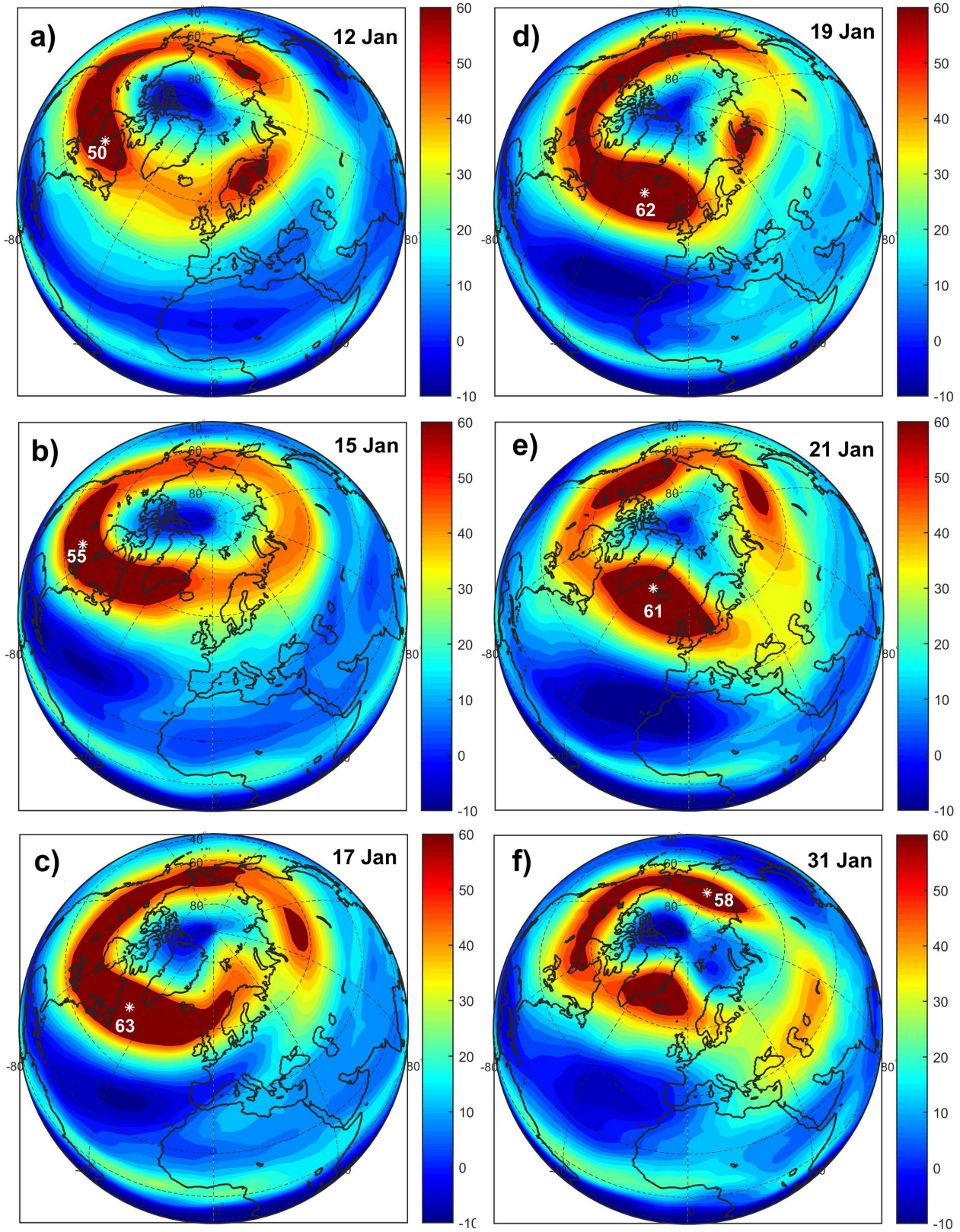
a)
12 Jan
50
d)
19 Jan
62
b)
15 Jan
55
e)
21 Jan
61
c)
17 Jan
63
f)
31 Jan
58
60
50
40
30
20
10
0
-10
40
60
80
-80

Fig. 2.

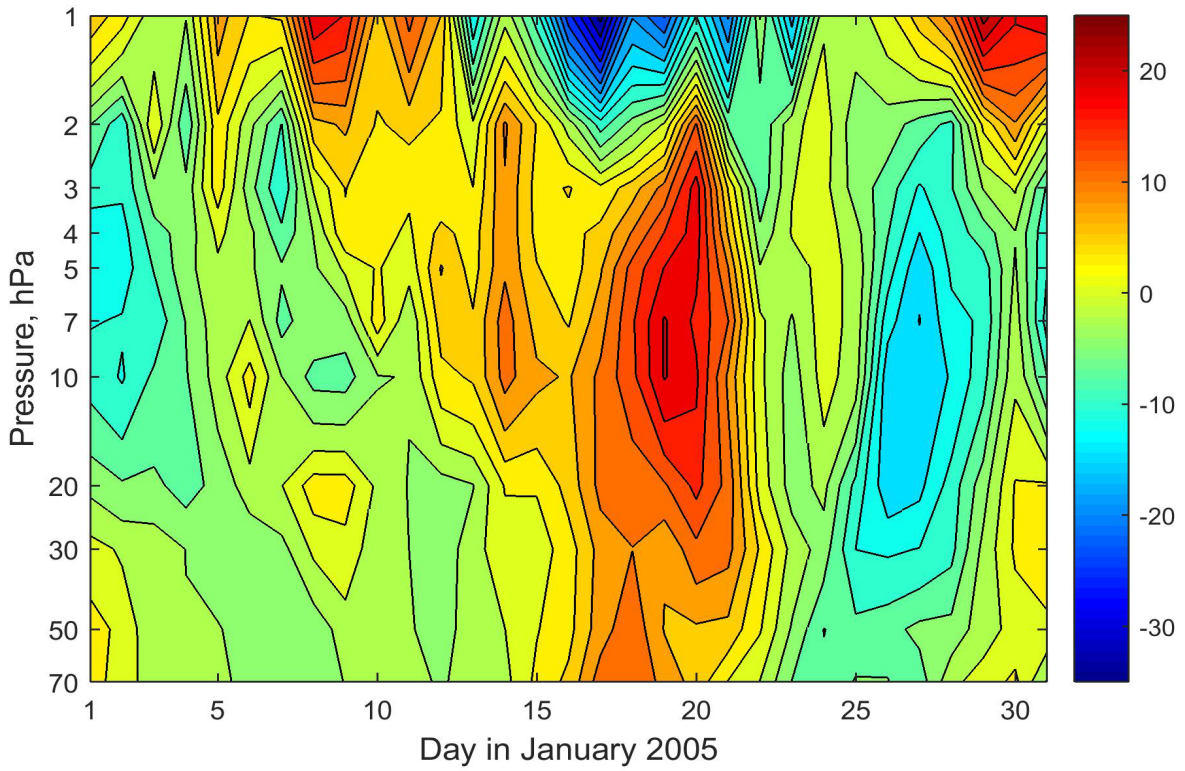
Pressure, hPa
1
2
3
4
5
7
10
20
30
50
70
1
5
10
15
20
25
30
Day in January 2005
20
10
0
-10
-20
-30

Fig. 3.

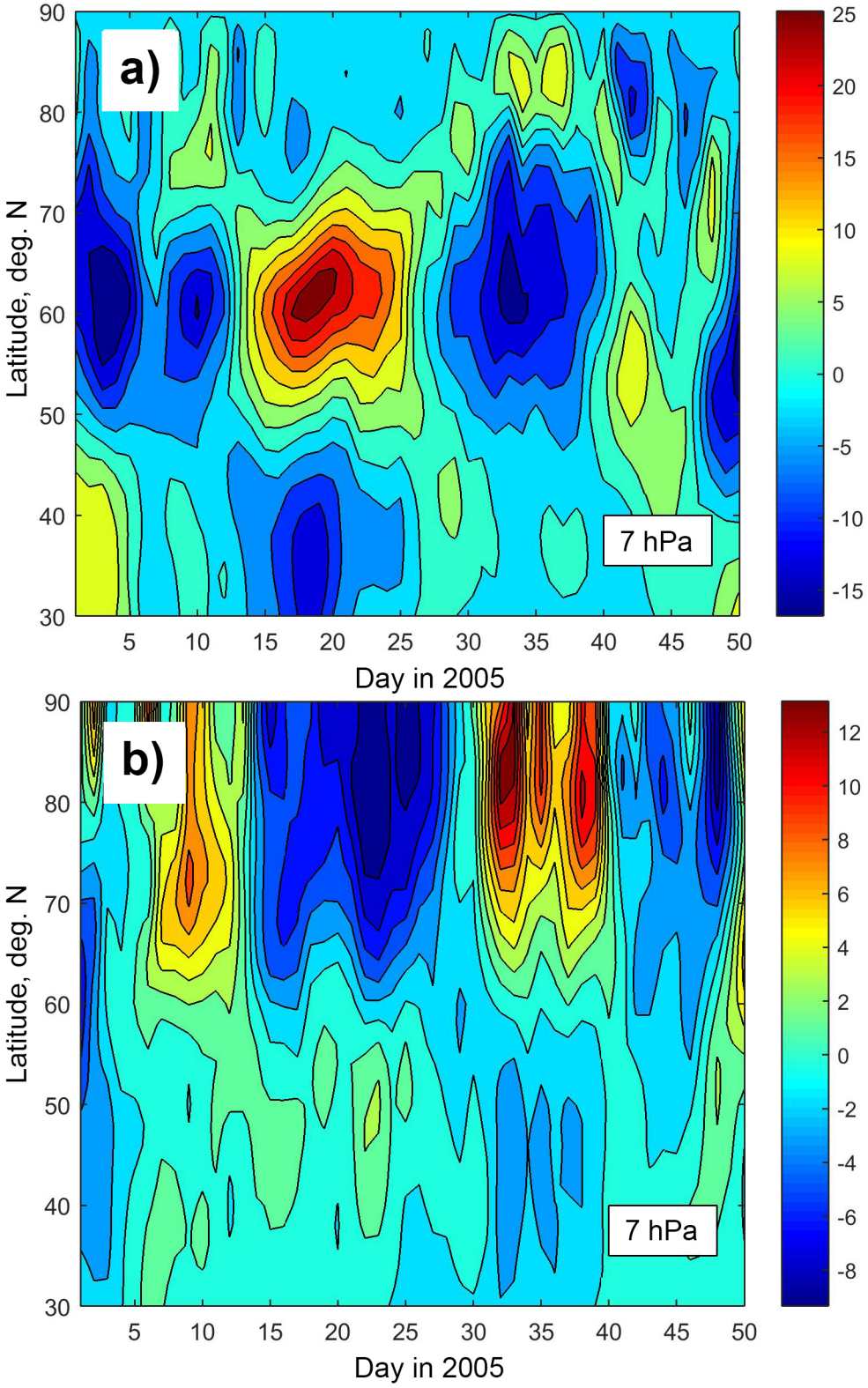
a)
7 hPa
Latitude, deg. N
Day in 2005
b)
7 hPa
Latitude, deg. N
Day in 2005

Fig. 4.

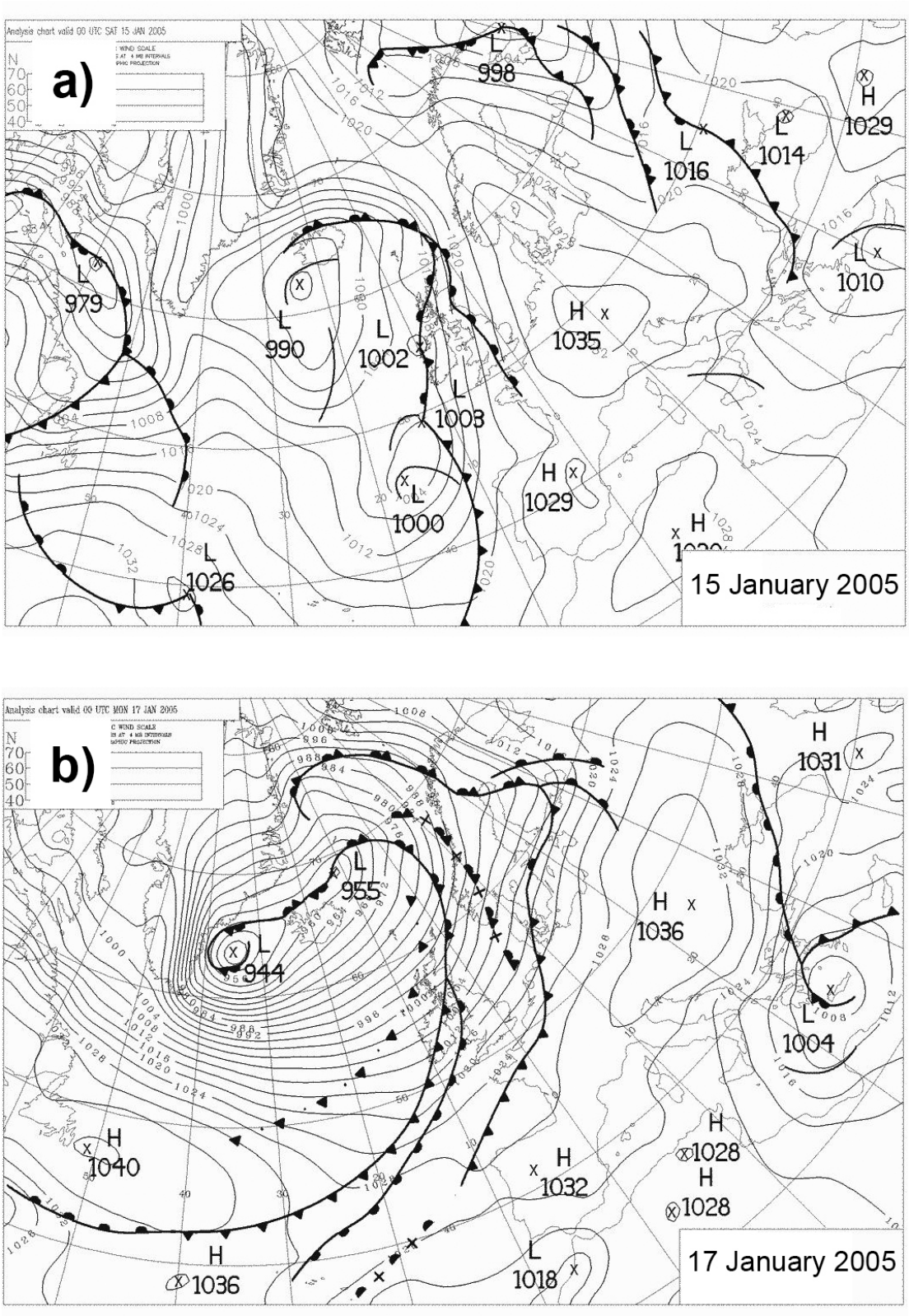
Analysis chart valid 00 UTC SAT 15 JAN 2005
a)
998
1029
1014
1016
1010
979
990
1002
1003
1035
1000
1029
1026
15 January 2005
Analysis chart valid 00 UTC MON 17 JAN 2005
b)
955
944
1031
1036
1004
1040
1032
1028
1028
1036
1018
17 January 2005

Fig. 5.

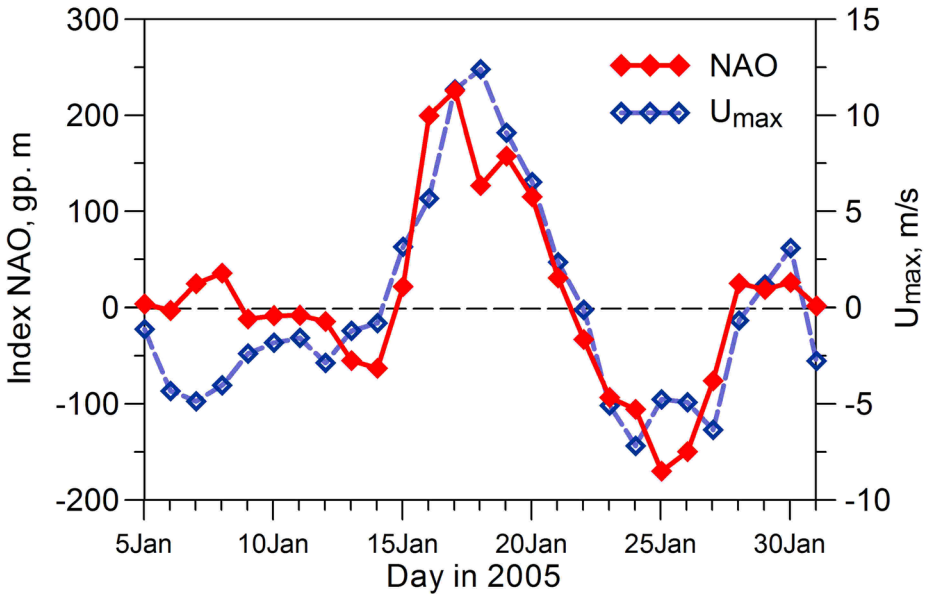
300
200
100
0
-100
-200
15
10
5
0
-5
-10
NAO
Umax
Index NAO, gp. m
Umax, m/s
5Jan
10Jan
15Jan
20Jan
25Jan
30Jan
Day in 2005

Fig. 6.

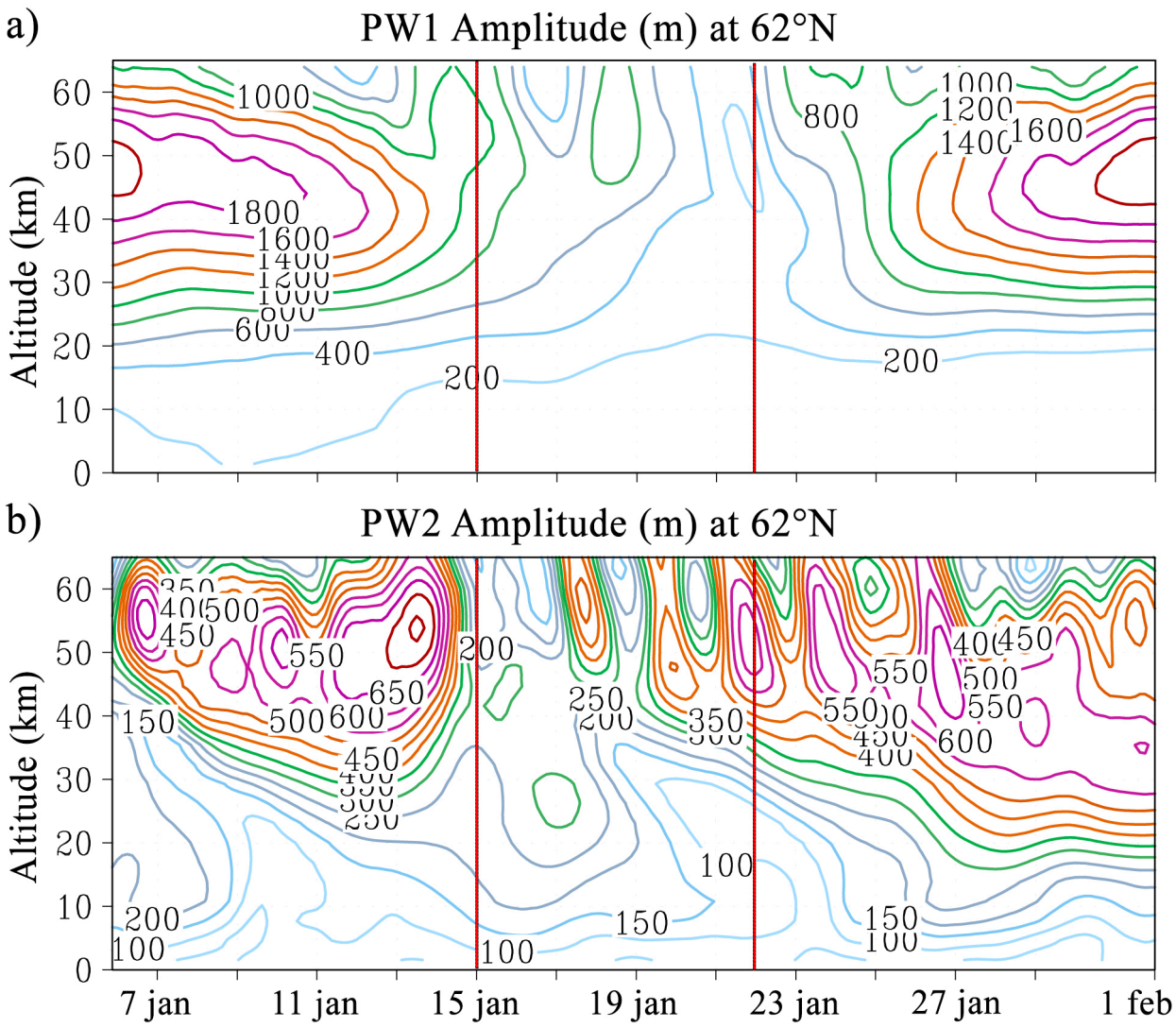
a)
PW1 Amplitude (m) at 62°N
Altitude (km)
b)
PW2 Amplitude (m) at 62°N
Altitude (km)
7 jan
11 jan
15 jan
19 jan
23 jan
27 jan
1 feb

Fig. 7.

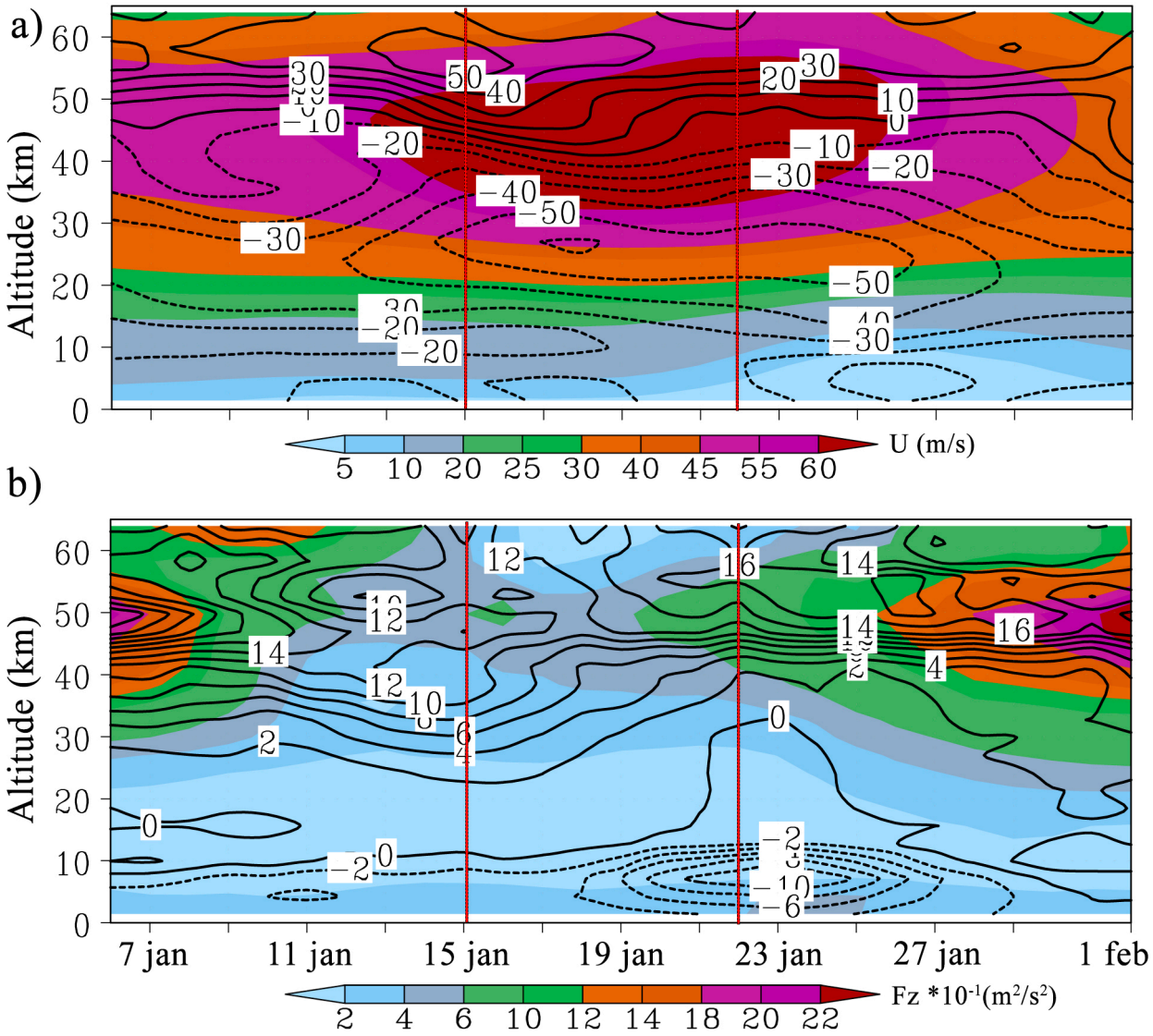
a)
Altitude (km)
60
50
40
30
20
10
0
30
50
40
20
30
10
−10
−20
−10
−30
−20
−40
−50
−30
−50
−20
−20
−30
5 10 20 25 30 40 45 55 60
U (m/s)
b)
Altitude (km)
12
16
14
12
14
16
14
4
12
10
6
2
0
0
−2
0
−2
−10
−6
7 jan
11 jan
15 jan
19 jan
23 jan
27 jan
1 feb
2 4 6 10 12 14 18 20 22
Fz *10-1(m2/s2)

Fig. 8.